Journal of Membrane Science, Volume 549, 1 March 2018, Pages 649-659
DOI:10.1016/j.memsci.2017.10.052

Selective-Exhaust Gas Recirculation for CO_2 Capture using Membrane Technology

Giuseppe Russo[1], George Prpich[2], Edward J Anthony[2*], F. Montagnaro[1], N. Jurado[2], G. Di Lorenzo[2], and Hamidreza G. Darabkhani[3]

[1] School of Polytechnic and Basic Sciences, University of Naples Federico II, 80126 Naples, Italy

[2]Centre for Combustion and CCS, Energy & Power Department, School of Water, Energy and Environment (SWEE), Cranfield University, Cranfield, Bedfordshire MK43 0AL, UK

3. Department of Engineering, Staffordshire University, College Road, Stoke-on-Trent, ST4 2DE, UK

* Corresponding author. E-mail address: b.j.anthony@cranfield.ac.uk

Abstract

Membranes can potentially offer low-cost CO_2 capture from post-combustion flue gas. However, the low partial pressure of CO_2 in flue gases can inhibit their effectiveness unless methods are employed to increase their partial pressure. Selective-Exhaust Gas Recirculation (S-EGR) has recently received considerable attention. In this study, the performance of a dense polydimethylsiloxane (PDMS) membrane for the separation of CO_2/N_2 binary model mixtures for S-EGR application was investigated using a bench-scale experimental rig. Measurements at different pressures, at different feeding concentrations and with nitrogen as sweep gas revealed an average carbon dioxide permeability of 2943 ± 4.1%$_{RSD}$ Barrer. The bench-scale membrane module showed high potential to separate binary mixtures of N_2 and CO_2 containing 5 to 20% CO_2. The permeability was slightly affected by feed pressures ranging from 1 to 2.4 bar. Furthermore, the separation selectivity for a CO_2/N_2 mixture of 10%/90% (by volume) reached a maximum of 10.55 at 1.8 bar. Based on the results from the bench-scale experiments, a pilot-scale PDMS membrane module was tested for the first time using a real flue gas mixture taken from the combustion of natural gas. Results from the pilot-scale experiments confirmed the potential of the PDMS membrane system to be used in an S-EGR configuration for capture of CO_2.

1. Introduction

Global warming is due to anthropogenic release of carbon dioxide and other polyatomic gases into the atmosphere [1]. Atmospheric CO_2 concentration has increased from 275 to

387 ppm over the past century and is currently around 407 ppm [2]. Combustion of fossil fuels (e.g., coal, oil, natural gas) for power generation is the leading source of increasing atmospheric CO_2 levels accounting for almost half the annual CO_2 emissions [3]. As power generation via fossil fuels produces cheap and reliable electricity, demand for them will continue over the short to medium term, hence solutions to mitigate the release of CO_2 are urgently needed [1].

Carbon capture and storage (CCS) is a family of technologies that offer the potential to mitigate CO_2 emissions [3]. Recent research on CCS technologies has been considerable as governments seek to reduce the carbon emissions released from power generation [4].

Strategies to reduce CO_2 emissions from power generation can be classified into three broad categories [3,5].

- Oxy-fuel combustion [6,7]: A concentrated oxygen feed is reacted with a fossil fuel (e.g., coal, gas, oil) to produce a highly-concentrated exhaust stream of CO_2. The exhaust stream can be recycled back into the fossil fuel burner, and ultimately the concentrated CO_2 stream is captured and stored.
- Pre-combustion [8–10]: A gasification process partially oxidises a fossil fuel (e.g., coal) under high temperature and pressure to generate a synthesis gas that can be reformed to produce CO_2 and hydrogen. The CO_2 can be recovered and the hydrogen-rich fuel used in the combustion process.
- Post-combustion [11,12]: A fossil fuel is combusted and CO_2 is removed from the flue gas.

Among these three strategies, post-combustion capture technologies have the key advantage that they can be retrofitted to existing plants [13]. Commonly studied approaches for post-combustion capture include absorption in liquids (e.g., monoethanolamine (MEA)) [14], adsorption onto solids (e.g., activated carbon) [15,16], cryogenic distillation [17], and membrane separation [18]. Carbon capture via chemical absorption using MEA or other amines is the most advanced technology, as it is well established in the gas industry, and a number of pilot and demonstration studies have been undertaken around the world to demonstrate its potential for use in CO_2 capture from power plant flue gas [19,20]. However, liquid amine absorption has several drawbacks. Energy requirements for regeneration of the solvent are considerable and result in overall power plant efficiency losses of 10-14% [21,22]. Moreover, solvent degradation due to secondary reactions, e.g., with SO_x, is another

issue that increases material replacement and disposal costs as well as contributing to environmental pollution [23].

Gas separation membranes compete well with liquid sorption technologies and have less environmental impact, and have a small technology footprint that can be more easily retrofitted to existing power plants with fewer modifications. Most importantly, compared to MEA and other amine systems, a multi-stage membrane system demands lower specific energy for separating CO_2 at low concentrations in flue gas [24].

Membrane gas separation is a pressure-driven process whereby the partial pressure difference between feed and permeate drives separation of target gas molecules across the membrane [25]. Industrial membrane gas separation processes have mainly focussed on nitrogen production, air drying [26] and natural gas treatment [27]. For CO_2 separation, membranes have been used to remove CO_2 from methane (CO_2/CH_4 separation), either for natural gas processing [28], or purification of recovered landfill biogas [29].

Despite these benefits, membrane systems remain untested at scale and a number of operational challenges must be overcome before successful integration with full-scale power plants can be realised. Particular challenges are gas composition, pressure, and temperature. Flue gas composition varies depending on the type of fossil fuel used and the method of combustion. Carbon dioxide content (by volume) can range from 4% for a gas turbine plant to 7-10% for a natural gas-fired boiler, to 15% for coal power plants [3]. This partial pressure difference will also influence CO_2 flux (drive) across the membrane, thus affecting separation performance. Measures to enhance the partial pressure driving gradient include: (1) increasing pressure on the feed side; (2) increasing CO_2 partial pressure in the feed gas (e.g., increasing CO_2 content of flue gas); and (3) enhancing CO_2 partial pressure gradient on the permeate side (e.g., using a sweep gas, or replacing the sweep gas with vacuum) [24]. Increasing or decreasing the carbon flux will often introduce an energy penalty, e.g., compressors or vacuum pumps [30]; however, solutions can be found to achieve benefits and mitigate energy penalties. An integrated solution might include exhaust gas recirculation [24] with membrane recovery, which increases the CO_2 content of the recycle stream. This approach generates a higher CO_2 content in the flue gas, which should benefit (operation and economics) subsequent final capture techniques (e.g., MEA). This type of integrated approach that uses selective-exhaust gas recirculation (S-EGR) has been described previously [31].

Research on scalable membrane systems is often focussed on simulation modelling of pilot-scale operations and membrane material performance, and for a review of research on novel membrane materials for recovery of CO_2 from flue gas, the interested reader can refer elsewhere [32–35]. Most lab-scale permeation studies characterise membrane performance under extremely well controlled conditions. Few studies currently explore the challenges of membrane application under practical conditions.

Feng and Ivory studied the separation of CO_2 from combustion flue gas using hollow fibre membranes [36]. Hagg et al. performed a numerical simulation of CO_2 separation from the flue gas generated from a power plant [37]. Favre et al. studied the energy input necessary to recover CO_2 from flue gas [38]. Unfortunately, less information is available on the use of sweep gas to recover CO_2 in a membrane unit. A techno-economic simulation investigating the influence of sweep gas on CO_2/N_2 membranes for post-combustion capture showed that using sweep gas in a cascade membrane system provided an energetic advantage over a cascaded membrane unit reliant on compression only [24]. Merkel et al. simulated a two-stage, two-step membrane system that combined a countercurrent flow regime and a vacuum to recover CO_2 from flue gas when the flue gas was used as the sweep gas [12]. They showed that sweep operation has the potential to lower the CO_2 capture energy penalty significantly, but that more than 50% of combustion air must be used as sweep to maximise energy savings. Similarly, Merkel et al. simulated the use of a S-EGR approach in a natural gas combined cycle and showed that the use of air as a sweep stream could provide low-cost CO_2 capture [39]. Similar results were obtained for a two-stage, two-step membrane system with air sweep for capturing CO_2 from a coal-fired power plant [40].

Despite these contributions, few studies show CO_2 separation via membrane at the pilot scale, and to the authors' knowledge fewer still studies provide experimental data on such systems. Here, we have explored the use of a membrane separation unit designed to recover, and recycle, CO_2 from the exhaust stream of a 100 kW natural gas-fired burner. The goal was to study the overall performance of the membrane-assisted S-EGR for CO_2 capture under challenging conditions appropriate for natural gas-fired plants.

Here, a polydimethylsiloxane (PDMS) membrane was used to separate CO_2 from CO_2/N_2 mixtures, with a bench-scale rig and these results (CO_2 permeation, selectivity, sweep gas/feed ratio) were then used to explore this concept in a pilot-scale unit.

2. Experimental Materials

2.1 Small-scale PDMS membrane

Experiments conducted at both bench scale and pilot scale used a PDMS membrane filter. The module used for the bench-scale studies was a Permselect PDMSXA-1.0 (Med Array Inc., USA), and the total available surface area of the membrane fibres was 1 m^2.

The PDMS membrane consisted of 12 600 hollow fibres bundled, contained within a polycarbonate housing, and sealed with a polyurethane resin. The module has an inlet and an outlet port for fluid communication with the inside of all the hollow fibres (also referred to as the tube and lumen side), and one inlet and two outlet ports for fluid communication to the outside of the hollow fibres (also referred to as the shell side).

Each fibre has an inside and outside diameter of 190 and 300 µm, respectively, and a wall thickness of 55 µm; the membrane's physical characteristics are given in Table 1.

Table 1. Structural characteristics of membrane module utilised

Membrane Material		PDMS (Silicone)
Membrane Type		Dense Hollow Fibre
Fibre ID	µm	190
Fibre OD	µm	300
Fibre Wall Thickness	µm	55
Fibre Count	#	12 600
Membrane Area	m^2	1.0
Module Length	m	0.14
Module Diameter	m	0.06
Fittings/Connection Size	in	Barbed "1/4"
Shell/End Caps		Polycarbonate
Fittings Material		Polycarbonate
Potting Material		Polyurethane
Other Materials of Construction		Polypropylene, Acrylic

2.2 Experimental Conditions

Gas measurements were obtained using a transportable multi-gas Fourier-Transform Infra-Red spectroscope (FTIR) analyser, Protir 204M (Protea, UK). The FTIR analyser uses nitrogen as the reference gas and has pre-loaded calibration methods for 28 gas species including CO_2, O_2, N_2 and H_2O.

A simulated gas feed was prepared by blending different molar ratios of CO_2 and N_2 and verifying composition using the FTIR analyser. During experiments, retentate and permeate streams were sampled a minimum of two times each to confirm composition. Finally, all gas flow rates were monitored using a series of rotameters. All fittings were comprised either of

stainless steel or plastic tubing. Gas for all bench-top studies was supplied via cylinders operating at 3 bar and CO_2 and N_2 purities were 99.9%.

2.3. Bench-top experimental configuration

Mixed gas permeation tests were conducted on a continuous flow membrane separation unit. The concurrent mode of operation was used for testing the membrane module. A schematic of the apparatus used is shown in Fig. 1

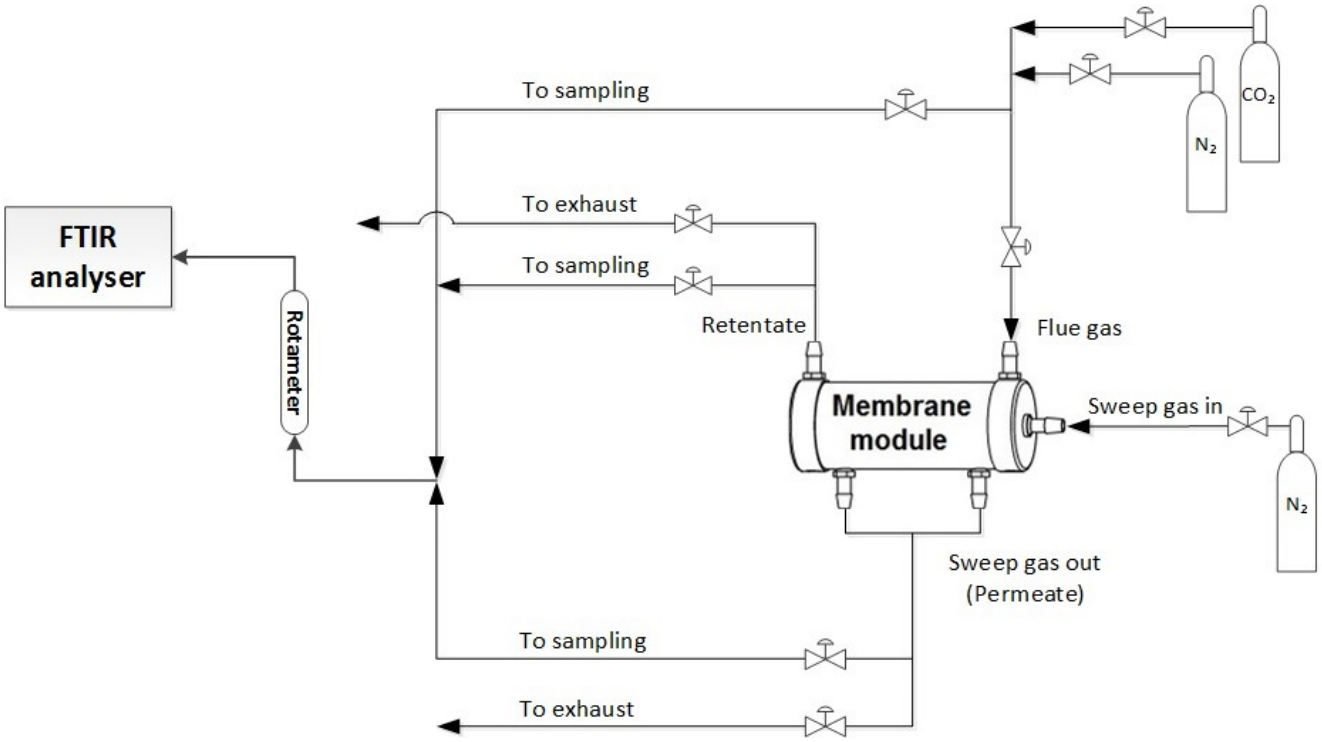

Fig. 1. Continuous flow setup using concurrent configuration and N_2 as sweep gas for CO_2/N_2 permeation tests

In order to identify the optimum incoming flow rates for the separation, recovery of CO_2 from the feed stream at different feed and sweep rates was studied. The sweep-to-feed flow ratio is defined as:

$$R_s = \frac{Q_s}{Q_f} \tag{1}$$

where Q_s and Q_f are the gas flow rates in the sweep and feed stream, respectively.

Preliminary tests were carried out by feeding 5 dm^3/min of a CO_2/N_2 gas mixture with the composition of 10/90% (by volume). Pure nitrogen was used as a sweep gas and was

supplied to the shell side of the membrane at different sweep-to-feed flow ratios. CO_2 recovery was investigated by varying the sweep flow rate from 2 to 10 dm^3/min. The flow rates were chosen according to the operating conditions suggested by the manufacturer.

The separation capability of the membrane was investigated by feeding different CO_2/N_2 mixtures with different compositions: 5, 10, 15, 20% (by volume) of CO_2 (see below). Furthermore, the permeation experiments were undertaken with feed pressures ranging from 1 to 2.4 bar in order to evaluate some key membrane properties. The sweep gas pressure was maintained at approximately 1 bar. Both air and 100% nitrogen were used as sweep gas. All experiments were carried out at room temperature (~21°C). Feed flow was introduced on the lumen side of the membrane with the sweep flow on the shell side. A back-pressure regulator on the retentate line allowed the required feed pressures to be applied in the module. The retentate and permeate flow rates were measured using a main rotameter before the FTIR analyser. Nevertheless, constant flow rates were maintained at ca. 10 dm^3/min on the feed and sweep side. All composition measurements were taken into account for the determination of the permeation parameters once the continuous system reached steady state.

To characterise the separation properties of the membrane various parameters were determined from the compositions, pressures and flow rate measurements. The permeability of a gas component i through the membrane was calculated as:

$$\mathrm{Pi} = \frac{\mathrm{Q_p\ y}}{\Delta \mathrm{p_{lni}\ A}}\ \mathrm{l} = \frac{\mathrm{N_i}}{\Delta \mathrm{p_{lni}\ A}}\ \mathrm{l} \qquad (2)$$

where P_i (Barrer) is the permeability of a gas component i, l (cm) the thickness of the dense layer, Q_p ($cm^3\ s^{-1}$) the gas flow rate in the permeate stream, A the effective permeation area and N_i (cm^3 (STP) $cm^{-2}\ s^{-1}$) the steady state flux of component i. A log-mean pressure drop (Δp_{lni}, cmHg) was used as the driving force according to the cross-flow design of the module studied and was defined as:

$$\Delta \mathrm{p_{lni}} = \frac{(\mathrm{p_{f,i}} - \mathrm{p_{s,i}}) - (\mathrm{p_{r,i}} - \mathrm{p_{p,i}})}{\ln[(\mathrm{p_{f,i}} - \mathrm{p_{s,i}})/(\mathrm{p_{r,i}} - \mathrm{p_{p,i}})]} \qquad (3)$$

where $p_{f,i}$, $p_{s,i}$, $p_{p,i}$ and $p_{r,i}$ are partial pressures for component i in feed, sweep in, permeate (sweep exit) and retentate (flue gas exit) sides, respectively. In this way, the permeability was expressed in units of Barrer (1 Barrer = 10^{-10} cm^3 (STP) cm cm^{-2} $cmHg^{-1}$ = 3.35 x 10^{-16} mol m m^{-2} s^{-1} Pa^{-1}).

Membrane selectivity was also estimated. Generally speaking, membrane selectivity is the relative permeability of different gas species in a mixture. For a binary mixture, the ideal membrane selectivity, $\alpha_{A/B}^{ideal}$ of component *A* over *B* can be calculated by determining the ratio of pure gas permeability for species A and B:

$$\alpha_{A/B}^{ideal} = \frac{P_A}{P_B} \tag{4}$$

In a binary mixture species A might affect the permeability of species B and in this case the separation membrane selectivity $\alpha_{A/B}^{sep}$ can be determined as the ratio of the permeabilities:

$$\alpha_{A/B}^{sep} = \frac{P_A}{P_B} = \frac{N_A/\Delta p_A}{N_B/\Delta p_B} \tag{5}$$

To complete the characterisation of the separation properties of the membrane the amount of gas captured from the feed stream was taken into account by introducing the recovery (also called recovery ratio) of the gas separated, defined as:

$$R = \frac{Q_p y}{Q f x} \tag{6}$$

where Q_p and Q_f are the gas flow rates in the permeate and feed stream, *y* and *x* the concentration of the permeant in the permeate (sweep out) and feed stream, respectively.

2.4. Pilot-scale materials and methods

The pilot-scale 100 kW CO_2 membrane rig facility employed in this study used a 100 kW MP4 Nu-Way burner fuelled with city natural gas and ambient air supplied by a centrifugal fan. Combustion gas mixture was controlled via an electronic gas proportional valve that maintained stoichiometric ratios. The rig was designed to operate in various modes (e.g., recirculation, recirculation with membrane, no recirculation) and for this reason it was equipped with two heat exchangers using cooling water, of which the second one was required to reduce the flue gas temperature to about 40°C before entering the membrane unit to avoid exceeding its maximum allowable temperature. A water removal system was also installed. The system is shown schematically in Fig. 2.

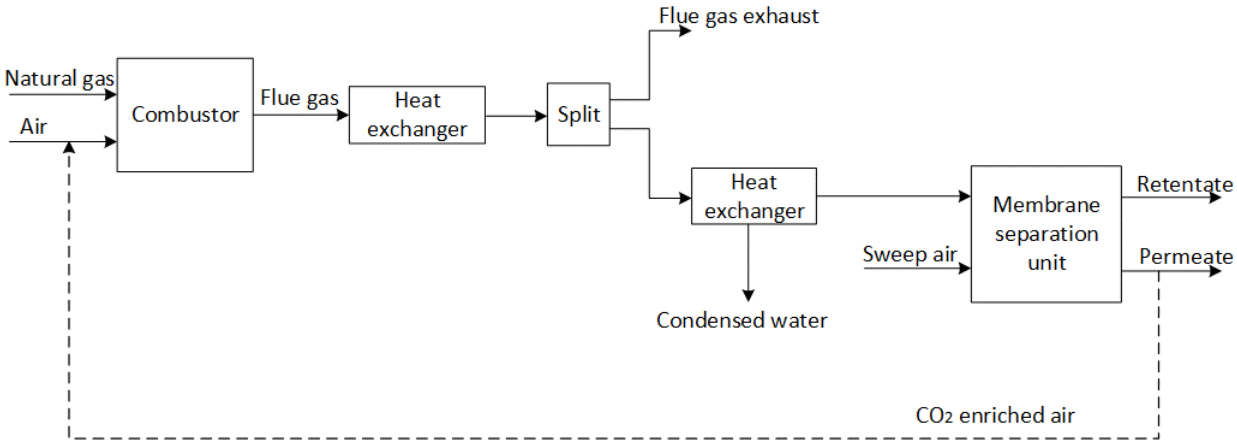

Fig. 2. Schematic representation of the pilot-scale rig

Fresh ambient air was used as the sweep gas and was provided via fan. Also, the flue gas entering the membrane module was moved by a small brushless fan. The separation unit used a PDMS hollow-fibre membrane module, NAGASEP GS-M20-35S (Nagayanagi Co. Ltd, Tokyo) of the following main specifications (Table 2):

Table 2. GS-M20-35S main specifications

Thickness of the hollow-fibre membrane	20 μm
Area of the hollow-fibre membranes	35 m^2
Number of hollow fibres	133 000
Outer measurements	230 mm (D) x 564 mm (L)

The module included both an inlet and an outlet port to enable fluid communication with the inside of all the hollow fibres (lumen side). It also had a single inlet and outlet port for fluid communication to the outside of the hollow fibres (shell side).

The system operated at atmospheric pressure. Orifice plates were used to calculate the flow rates. Thermocouples were used to measure the temperature of the gases at each membrane inlet. Differential pressure meters were used to measure the pressure drop within the system.

Flue gas and sweep air mass rates were calculated from the flow rates as determined by the orifice plates. The global mass balance for the system as well as the partial mass balance (e.g., on CO_2) were determined, to enable calculation of the retentate and permeate mass flow rates, using:

$$\begin{cases} F_{IN} + S_{IN} = F_{OUT} + S_{OUT} \\ F_{IN} \cdot x_{IN} + S_{IN} \cdot y_{IN} = F_{OUT} \cdot x_{OUT} + S_{OUT} \cdot y_{OUT} \end{cases} \quad (7)$$

where:

F_{IN} is the mass flow rate of the flue gas; F_{OUT} is the mass flow rate of the retentate; S_{IN} is the mass flow rate of the sweep air; S_{OUT} is the mass flow rate of the permeate; while x and y are the corresponding mass fractions for a generic component (e.g., CO_2).

3. Results and Discussion

In this section the results for the bench-scale experiments are reported in terms of CO_2 recovery for different sweep-to-feed flow ratio, permeability of CO_2 and N_2 as a function of feed pressure and membrane selectivity for CO_2/N_2. Similar to the bench-scale case, the membrane performance in the pilot-scale experiments was evaluated in terms of permeability and selectivity of the PDMS membrane to CO_2 and CO_2 recovery.

3.1 Bench-scale experiments

3.1.1 Influence of sweep-to-feed flow ratio on CO_2 recovery

The first set of experiments analysed the effect that the sweep-to-feed flow ratio had on the membrane's capability to recover CO_2 from a feed stream composed of binary mixtures of CO_2 and N_2. Pure nitrogen was used as a sweep gas.

Results describing the recovery of CO_2 from the feed stream are shown in Fig. 3; this set of tests used a concurrent configuration, a feed pressure of 1 bar, concentration of CO_2 in feed of 10%, flowrate of feed of 5 L/min, and pressure of the sweep gas of 1 bar. They show that the performance of the system was influenced by the variation of the sweep-to-feed flow ratio. From an operational perspective, CO_2 recovery reached a point of diminishing return at a sweep-to-feed flow ratio of about 1. Operation below this sweep ratio results in significantly reduced CO_2 capture, while operation above this ratio causes a significant increase of power input vs. amount of CO_2 captured, in agreement with an earlier study [39]. Research has shown that the use of a vacuum, rather than a sweep gas, will increase the partial pressure gradient across the membrane leading to better rates of CO_2 recovery [12]. Despite this, the use of a sweep gas was preferred in this study because of the use of the permeate stream to enrich the incoming combustion air in the exhaust gas recirculation system.

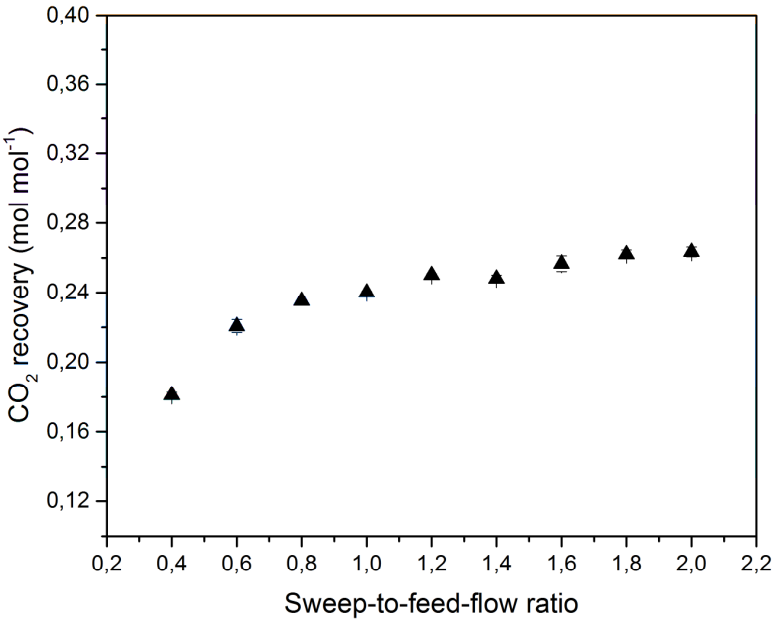

Fig. 3. CO_2 recovery at different sweep-to-feed-flow ratios (Temperature = 21°C, flowrate of feed = 5 L/min, CO_2 concentration in the feed stream = 10% and using pure N_2 as the sweep gas)

Sorption of CO_2 onto the membrane is driven by pressure. Therefore, the effect of changing the feed-side pressure on the permeability of the PDMS membrane was investigated by varying it from 1 bar to 2.4 bar, setting the flow rates from both sides at 10 L/min and keeping the remaining operating conditions the same as described for the aforementioned set of tests.

The mean values of the permeability coefficients for CO_2 and N_2 were estimated to be 2943 ± 4.1%$_{RSD}$ and 295 ± 12.8%$_{RSD}$ Barrer, respectively. This calculation assumed a membrane contact area of 0.63 m^2 (determined by the inner diameter of the fibres). The inner membrane area was used for these calculations, instead of the outer membrane area, because permeating flow was from the lumen side of the fibres outwards. Furthermore, permeability has been shown to be independent of the feed regime (via shell or lumen side) [41].

Silicone rubber membranes, like PDMS, have been used in various gas separation processes and many studies have assessed the performance of CO_2 and N_2 separation (e.g., [42–44]). The calculated permeability values are in good agreement with those determined in similar studies reported in the literature. Merkel et al. [43] studied the permeability of pure N_2 and CO_2 in rubbery PDMS material through a membrane cell, at a

temperature of 23°C, a feed pressure of 1.38 bar and using vacuum. The authors calculated permeabilities of 380 and 3200 Barrer for N_2 and CO_2, respectively. Similar results were observed by Jha et al. who reported a pure gas permeability of CO_2, at 20°C and a differential pressure of 1.033 bar, of 2645 Barrer [42]. Other studies, using similar systems and working with CO_2/H_2 mixtures, calculated CO_2 permeability in PDMS membranes of 2680 [41] and 2848 Barrer [45]. Most studies, however, were conducted using pure gas streams under highly controlled conditions and, thus, represent a best-case scenario. Though these permeability values can be used to estimate membrane performance at scale-up, it is unclear what effect gas mixtures might have on CO_2 permeability and thus recovery in a real system.

3.1.2 Effect of feed pressure on CO_2 separation performance

Experiments with varying differential pressure across the membrane (from 0 to 1.4 bar) were performed to determine the effect of feed pressure on CO_2 separation. The remaining operating conditions were set up as follows: flowrate of feed = 10 L/min, flowrate of sweep = 10 L/min, feed/sweep ratio = 1. The membrane unit has an upper pressure limit of 3 bar, after which the membrane unit might suffer irreversible damage. A binary mixture of CO_2 and N_2 at a ratio of 10/90 (by volume) was supplied to the lumen side and N_2 used as the sweep gas. Results showing the change in partial pressure of carbon dioxide in the retentate and permeate streams for each measurement are included in Fig. 4.

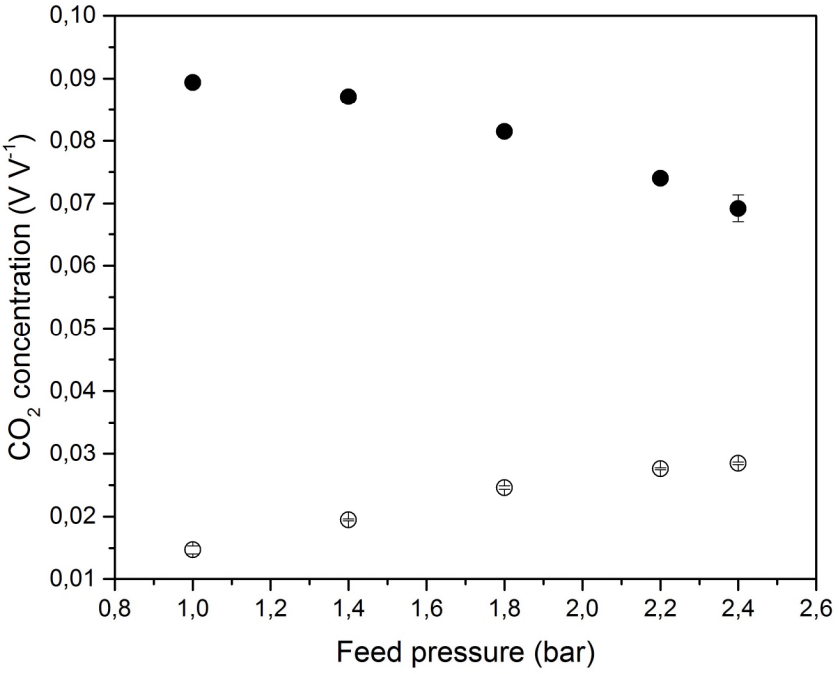

Fig. 4. Carbon dioxide concentration at different pressures evaluated in retentate (●) and permeate (○) (Temperature = 21°C, sweep/feed ratio = 1, flowrate of feed = 10 L/min, CO_2 concentration in the feed stream = 10% and using pure N_2 as the sweep gas)

It is evident from Fig. 4 that increased recovery of CO_2 occurred with increasing feed pressure. Carbon dioxide concentration is reduced with increasing feed pressure in the retentate, decreasing by about 14% under a feed pressure of 1 bar and by about 35% under 2.4 bar, while in the permeate the opposite behaviour was observed. Hence, the results indicate that CO_2 was enriched in the permeate stream, reaching a final concentration of about 0.03 (V V^{-1}) under a feed pressure of 2.4 bar. This relationship with a degree of proportionality between concentration and pressure applied has been observed previously in rubbery dense polymers [46,47]. Also in these studies, it was observed that when higher pressure is applied to the membrane, the concentration of the different permeated species is also higher. Therefore, improvements in CO_2 separation from a feed stream could be achieved by increasing the operational pressure across the membrane system, but at scale-up, this will come with the added cost of compressing the gas [12].

The effect of varying the pressure of the feed stream on CO_2 and N_2 permeability was also analysed (Fig. 5). The remaining operating conditions used for these tests were: feed/sweep ratio = 1, flowrate of feed = 10 L/min, pressure of sweep = 1 bar.

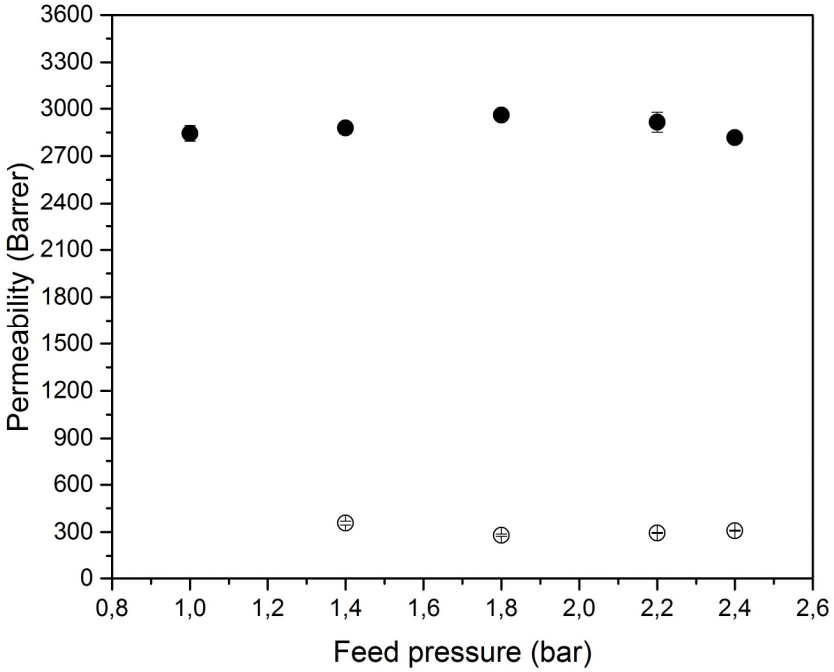

Fig. 5. Effect of feed pressure on CO_2 (●) and N_2 (○) permeability (Temperature = 21°C, sweep/feed ratio = 1, flowrate of feed = 10 L/min, CO_2 concentration in the feed stream = 10% and using pure N_2 as the sweep gas)

As expected, no significant effect on membrane permeability was observed (Fig. 5). Others have observed similar behaviour, for example Sadrzadeh et al. [48] describe a similar phenomenon. In their work they show that this behaviour is due to the influence of three factors: plasticisation, penetrant solubility and hydrostatic pressure. Taking into account the low pressures reached, plasticisation is negligible. The behaviour found is explained because the polymer could be compacted or compressed with increasing pressure, resulting in diffusivity of the molecules being affected. Therefore, as it was explained also by Ramírez-Morales [47], results obtained may be imputed to the effect of polymer compression on the solution-diffusion mechanism, where permeability is described as the product of diffusion (*D*) and solubility (*S*) coefficients in the membrane material. Generally speaking, as is shown in Table 3, due to the smaller kinetic diameter, the diffusivity of N_2 is higher than that of CO_2. Conversely sorption capability of CO_2 in dense PDMS is greater than that of N_2 because of its higher critical temperature and, consequently, it is more easily condensed (Table 3) which was confirmed by the experiments, where CO_2 permeability was found to be higher than that of N_2. Here we are assuming that the differences in operational temperature of 21 and 35ºC are not significant in terms of the behaviour of the two gases.

Table 3. Solubility and diffusivity of N_2 and CO_2 at 35°C

Pure gas	Critical temperature (K)	Kinetic diameter (nm)	D x 10^5 (cm^2/s)	S x 10^2 (cm^3 (STP)/ (cm^3(polym.) cmHg)
N_2	126.2	0.344	4.00	0.118
CO_2	304.21	0.363	2.63	1.74

Data obtained from [49–51]

Nevertheless, for N_2 the solubility is quite independent of pressure, and diffusivity decreases slightly with the increase of pressure due to the hydrostatic compression of the rubber membrane [50]. Conversely, the CO_2 solubility increases with high pressure, and its diffusivity decreases less than that of N_2 with pressure [49,50]. From these considerations and taking into account the low differential pressures across the membrane (from 0 to 1.4 bar) permeability of CO_2 and N_2 were expected to be only slightly affected and this was confirmed by the results illustrated in Fig. 5.

3.1.3 Separation selectivity

The effect of operating pressure on the permeation properties of the PDMS membrane unit was characterised using bench-scale testing. The potential application of the PDMS polymer as a separation membrane depends upon the permeate flux and the selectivity towards the gas to be separated. To characterise the separation performance of a CO_2/N_2 mixture, the permeability values shown in Fig. 6 must be discussed along with other factors such as separation selectivity. The separation selectivity at different feed pressures was studied, also looking at the corresponding recovery.

Fig. 6 shows the established separation selectivity and the CO_2 recovery at different feed pressures.

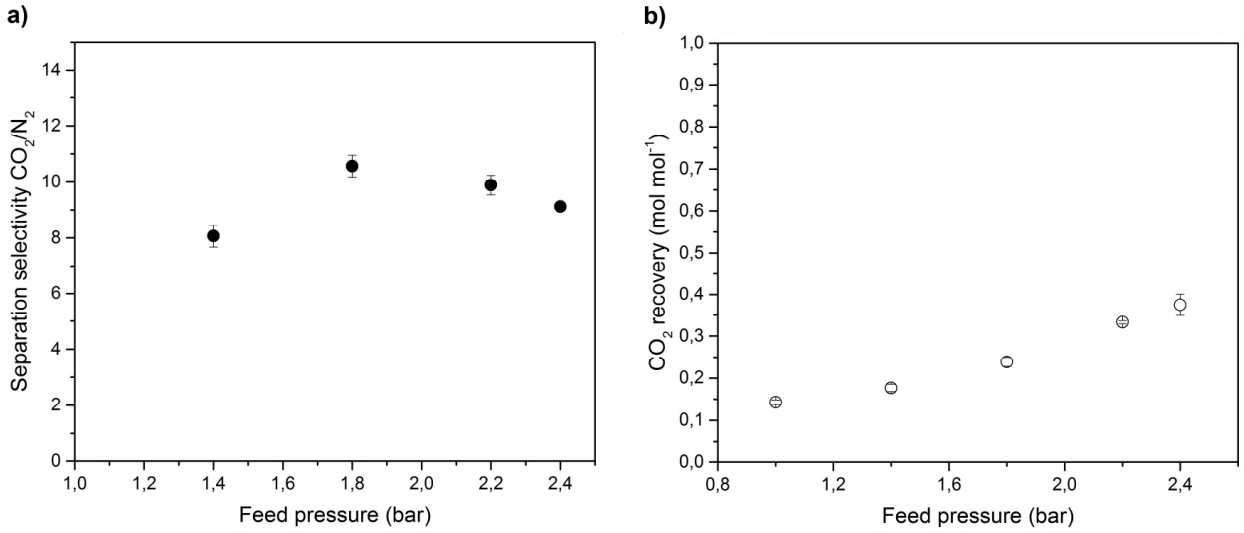

Fig. 6. Separation selectivities (6-a) for CO_2/N_2 mixture and CO_2 recovery (6-b) at different pressures (Temperature = 21°C, sweep/feed ratio = 1, flowrate of feed = 10 L/min, CO_2 concentration in the feed stream = 10%, and using pure N_2 as the sweep gas)

Previously it has been shown that the permeability of CO_2 through PDMS was higher than the permeability for N_2. Based on this observation, a higher selectivity of CO_2 over N_2 was expected: the results obtained showed this behaviour (Fig. 6) with separation selectivity reaching a maximum of 10.55 at 1.8 bar. Jha et al. studied CO_2 ideal selectivity at different temperatures and different differential pressures (between feed and sweep pressure) [42]. They found, at 20°C with a feed pressure of 1.846 bar and differential pressure of 1.033 bar, an ideal selectivity of 10.8. Similar values were found by Yeom et al. who used a PDMS membrane cell and carried out experiments on pure and CO_2/N_2 mixed gases [44]. They used a 20%/80% (by volume) CO_2/N_2 mixture, and found separation selectivity around 11.5 at 30°C. Given the ideal nature (i.e., pure gas) of the those studies, and the similarities between our collective permeabilities, it can be concluded that different constituent gas species in mixture will have a limited effect on the diffusion of CO_2 across the PDMS membrane. This observation is important when considering the separation of CO_2 from a complex gas mixture.

From the comparison of the results shown in Fig. 6, it seems that there is a positive effect of pressure on the performance of the membrane taking into account the achievable CO_2 recovery and the separation selectivity determined.

Flue gas exits from a natural gas combustor at relatively low pressures such that this pressure may not drive membrane separation processes. In the present work, permeation tests were conducted under mild conditions (using low pressures in a narrow range),

considering the objective of a practical membrane involved in the separation of CO_2 from flue gas of a natural gas combustor.

The effect of CO_2 concentration as a function of feed pressure is shown below in Fig. 7 to Fig. 9. As can be seen in these figures, permeabilities of carbon dioxide at a certain value of pressure, slightly increased with CO_2 feed concentration. In particular, permeabilities of CO_2 were around 2800 Barrer at 5% CO_2 feed concentration, around 2900 at 10%, and around 3000-3100 at 15 and 20%. As shown elsewhere [52], higher concentrations of carbon dioxide in the feed stream correspond to higher pressure drive force across the membranes. Furthermore, the trend of separation selectivity is similar for all conditions investigated, showing the highest value over the feed pressure range of 1.8-2.2 bar.

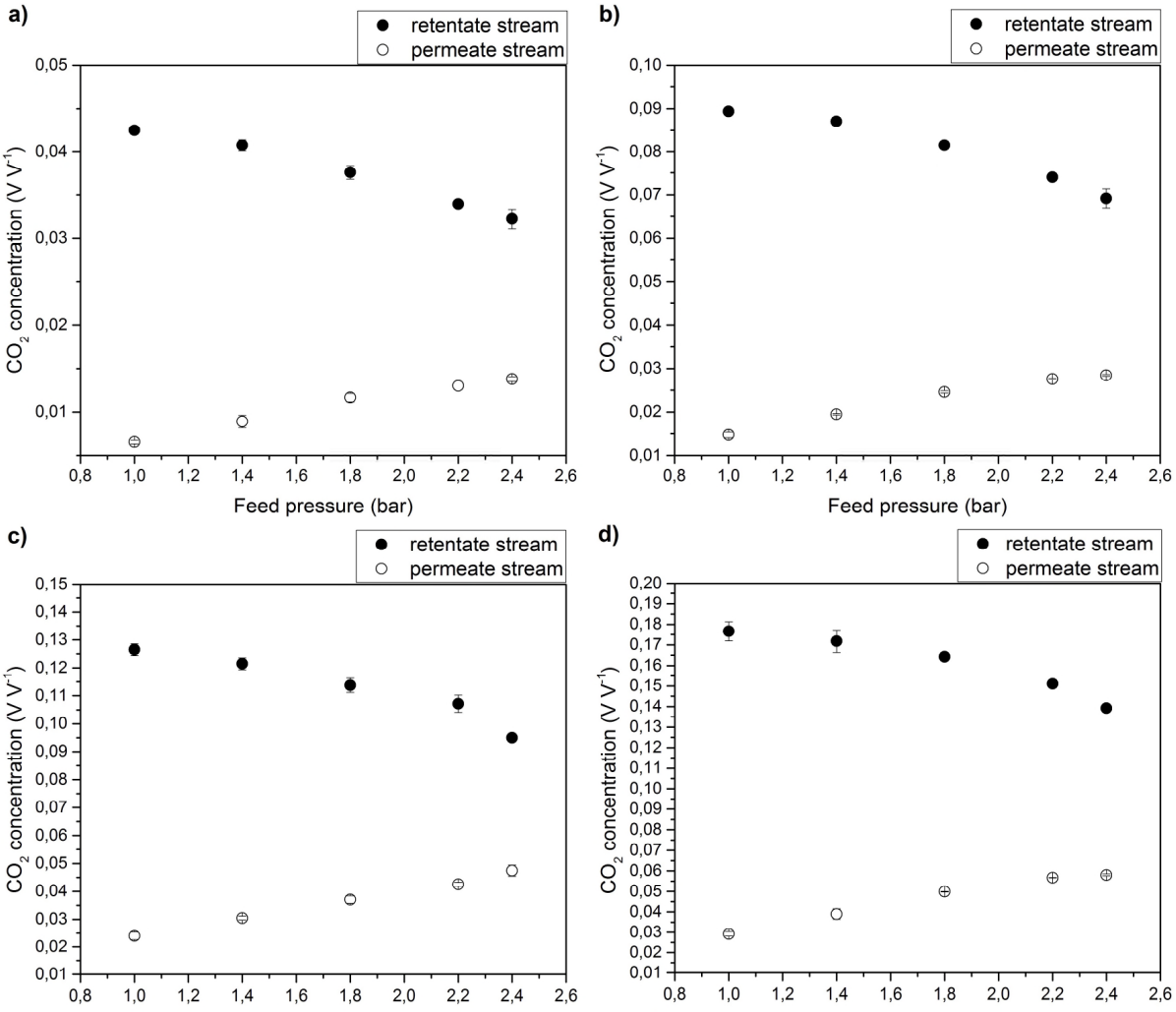

Fig. 7. CO_2 concentrations obtained using different CO_2 inputs (v/v): 5% (7-a), 10% (7-b), 15% (7-c) and 20% (7-d). (Temperature = 21°C, sweep/feed ratio = 1, flowrate of feed = 10 L/min, and using pure N_2 as the sweep gas)

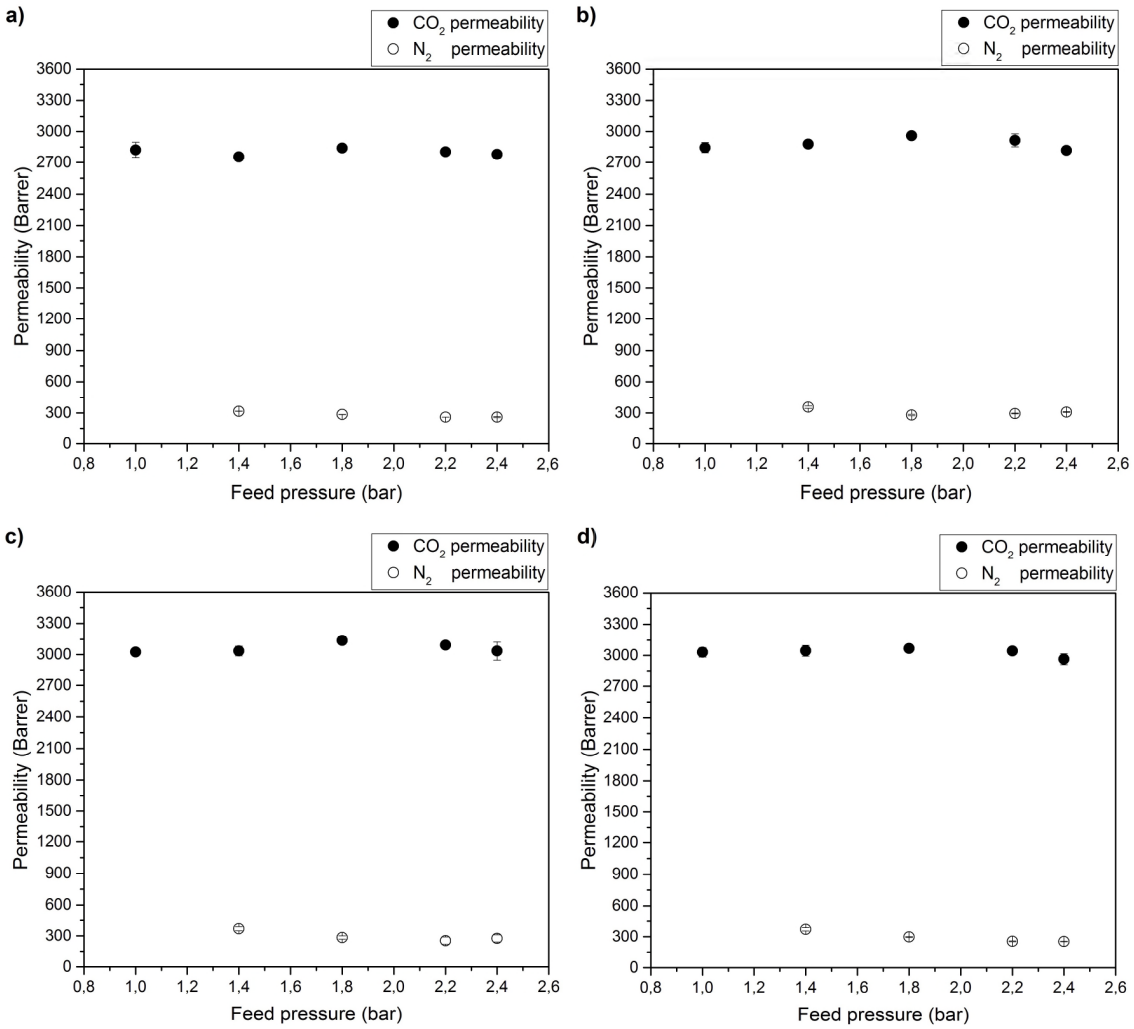

Fig. 8. Permeability measured using different CO_2 inputs (v/v): 5% (8-a), 10% (8-b), 15% (8-c) and 20% (8-d). (Temperature = 21°C, sweep/feed ratio = 1, flowrate of feed = 10 L/min, and using pure N_2 as the sweep gas)

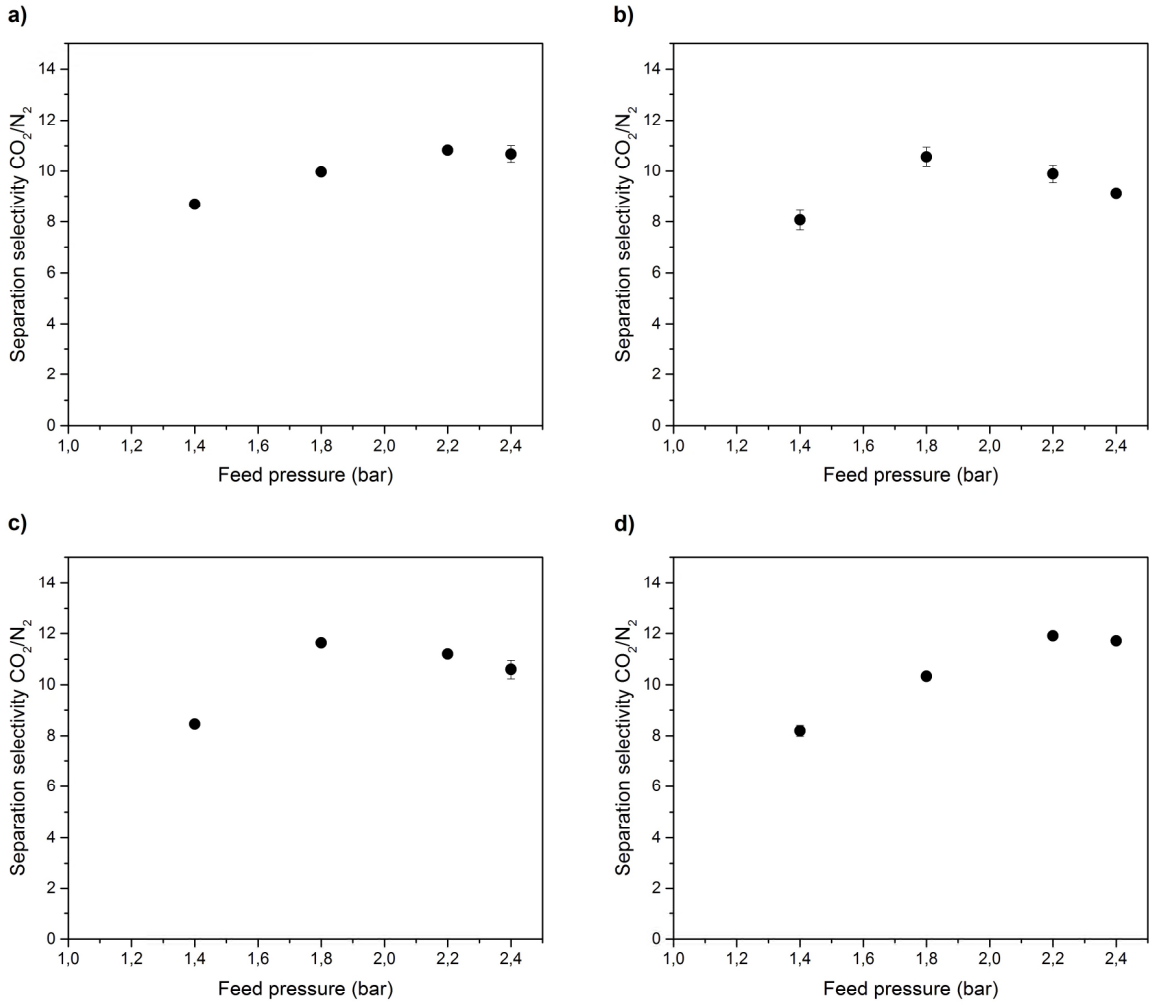

Fig. 9. Separation selectivity observed using different CO_2 inputs(v/v): 5% (9-a), 10% (9-b), 15% (9-c) and 20% (9-d). (Temperature = 21°C, sweep/feed ratio = 1, flowrate of feed = 10 L/min, and using pure N_2 as the sweep gas)

3.1.4. Transport of oxygen across the membrane

Additional experiments were run using air instead of nitrogen as the sweep gas to further study the influence of potentially competing gas species in the mixture. Fig. 10 shows the CO_2 and O_2 concentrations in the retentate and permeate at different feed pressures. These results were obtained by operating under the same conditions as in previous experiments where pure nitrogen was deployed as the sweep gas, with a 10%/90% (by volume) CO_2/N_2 mixed feed.

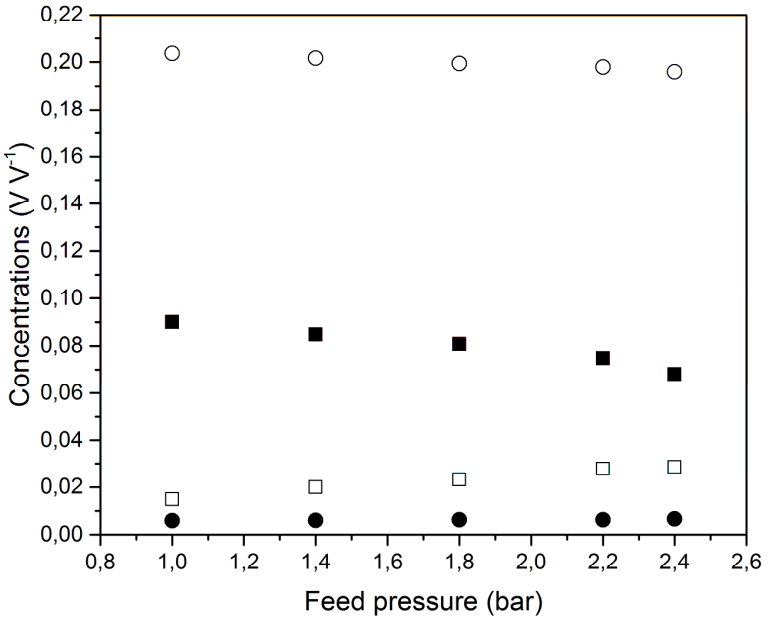

Fig. 10. CO_2 concentration in retentate (■) and in permeate (□); O_2 concentration in retentate (●) and in permeate (○) at different feed pressures. (Temperature = 21°C, sweep/feed ratio = 1, flowrate of feed = 10 L/min, and using pure air as the sweep gas).

The measurements show that CO_2 concentration in the retentate stream is only slightly affected by O_2 transport, and the CO_2 concentrations are quite close to those of the experiments with pure nitrogen sweep gas. The O_2 concentration in the retentate stream is around 0.006 (by volume) in each test. Besides, taking into account the lack of oxygen in the feed stream, it is possible to conclude that among all experiments the driving force (differential O_2 pressure between feed and sweep side) across the membrane is effectively the same. In fact, the amount of O_2 crossing the membrane from the sweep to the feed side is small compared to the CO_2 transfer as shown in Fig. 11a.

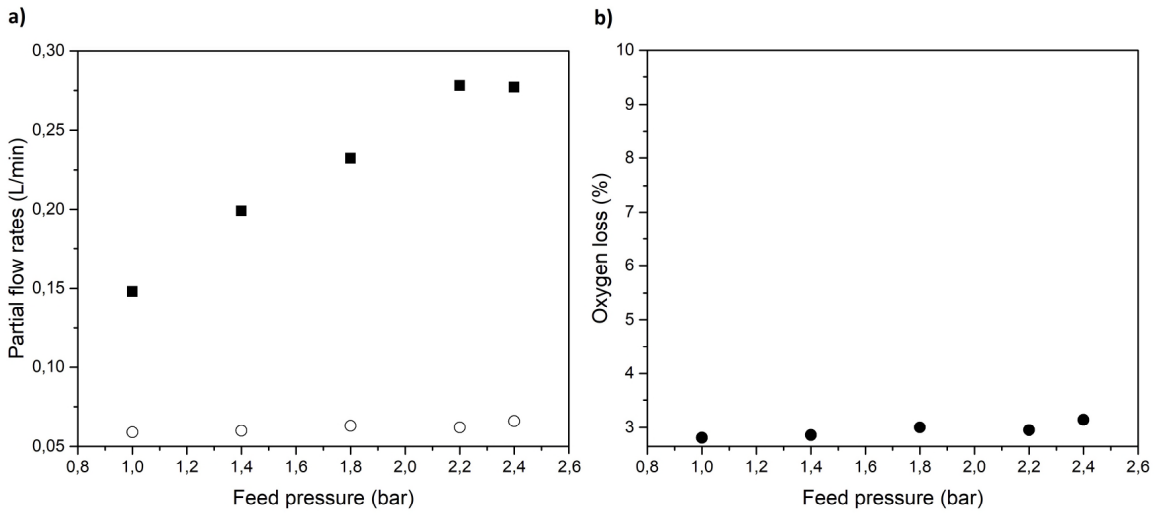

Fig. 11. a) O_2 flow rate from sweep air to feed side (○); CO_2 flow rate from feed to sweep side (■); b) O_2 loss from incoming sweep air (●) (Temperature = 21°C, sweep/feed ratio = 1, flowrate of feed = 10 L/min, and using pure air as the sweep gas)

Considering the potential use of the sweep air as the combustive agent for the boiler (S-EGR system), although a very small portion of the oxygen present in the sweep stream passes to the retentate, this aspect must be carefully evaluated for specific cases. For the experimental setup and operating conditions used for the present work (bench scale, ideal mixture of flue gas, etc.), the loss of oxygen leaving the sweep air stream has been estimated to vary between 2.8% (at 1 bar feed pressure) and 3.1% (at 2.4 bar feed pressure) as can be observed in Fig. 11b.

3.2 Pilot-scale rig

Using the results obtained from the bench-scale study, the same experiments were repeated in the pilot-scale rig using a real flue gas mixture from the combustion of natural gas.

The experiments were carried out after the flue gas concentrations reached steady state. The flue gas average composition and the sweep air composition are illustrated in Table 4. Minor species (e.g., NO_x) were not taken into account for the present study.

Table 4. Operating conditions for pilot-scale tests and major species composition in the main streams

Operating conditions	Sweep air	Flue gas (FG)	Permeate (Sweep out)	Retentate (FG out)
$T_{average}$ (°C)	30	40	30	29
$P_{average}$ (bar)	1.04	1.02	1.01	0.30
Flow rate (kg/h)	11.2-48.6	11.2	9.9-46.2	12.5-13.6

Composition major species (mol %)				
O_2	20.1-22.4	2.5-5.2	18.3-21.3	5.4-7.8
H_2O	0.7-1.1	3.4-9.9	1.9-3.5	1.8-4.6
N_2	76.9-78.9	78.1-81.0	75.6-77.4	77.7-84.0
CO_2	0.0	8.7-13.5	0.5-1.8	5.4-10.6

Based on findings from our bench-scale studies, the pilot testing began with a sweep-to-feed flow ratio of approximately 1. Furthermore, to simulate the capability for the membrane system to enrich the selective exhaust gas recirculation stream, a portion of the flue gas was diverted to the membrane system. The effect of sweep-to-feed flow ratio was assessed within a range of 1-4.43.

Fig. 12 shows the carbon dioxide concentrations in the retentate and permeate stream at different sweep-to-feed flow ratios.

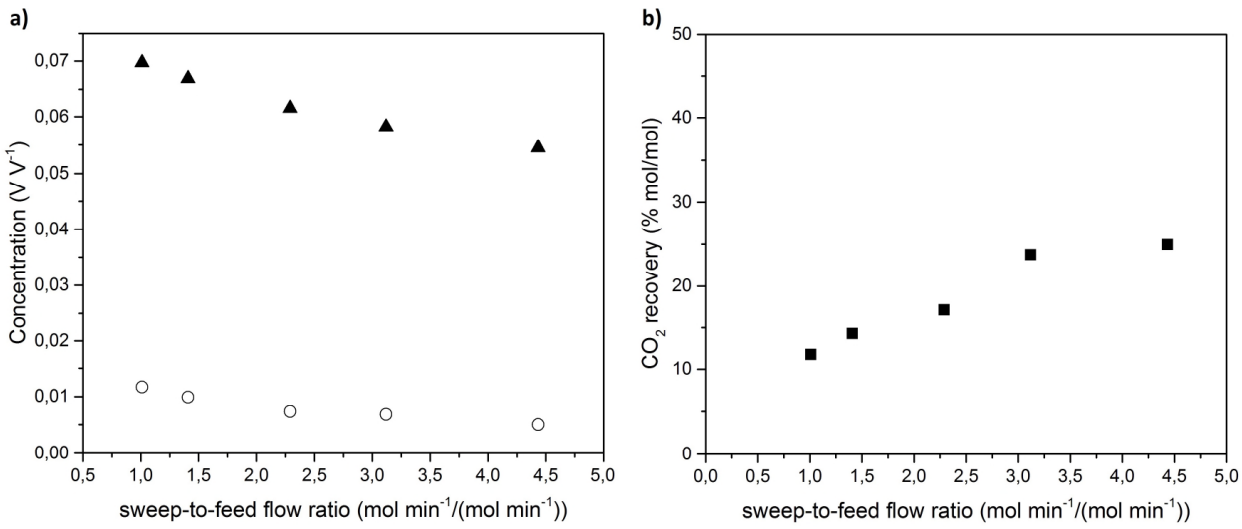

Fig. 12. Carbon dioxide concentrations at different sweep-to-feed flow ratios evaluated in retentate (▲) and permeate (○) (a), and carbon dioxide recovery at different sweep-to-feed flow ratios (b). (Temperature = 30-40°C, Feed pressure = 1.02 bar, Sweep/feed ratio = 1-3, flowrate of feed = 11.2 kg/h, using air as sweep gas)

Predictably, the CO_2 concentration in the permeate stream decreased moderately with the increased sweep-to-feed flow ratio, reaching low values as a consequence of the low driving force (differential partial pressures). The lowest permeate CO_2 concentration (0.5%) was found at the sweep-to-feed flow ratio of 4.43 and the highest (1.2%) was found at 1, as shown in Fig. 12. The retentate CO_2 concentration decreased with the lowest value (5.45%) found at the sweep-to-feed flow ratio of 4.43. Furthermore, the CO_2 recovery increased with the increased sweep-to-feed flow ratio as shown in Fig. 12. The results clearly showed a trade-off relationship between the CO_2 concentrations in the retentate and permeate, and CO_2 recovery. This relationship turned out to be advantageous for the CO_2 concentration in

the retentate. Nevertheless, only a comprehensive assessment of the whole separation process (including the process efficiency, costs, the flue gas flow rate to be treated, as well as the sweep air to use as CO_2-enriched combustion air) could allow us to make the choice of an optimal sweep-to-feed flow ratio. For instance, in the current study, a sweep-to-feed flow ratio of around 3 could be used to provide the approximate best-case scenario for CO_2 recovery.

In the investigation of the separation performance, other species in the system should be taken into account. Nevertheless, the operating conditions (e.g., different temperatures for the retentate and sweep streams) and the instruments used, did not allow us to properly calculate separation properties such as permeability and selectivity of components. In Fig. 13 water vapour and oxygen concentrations in the retentate and permeate are illustrated.

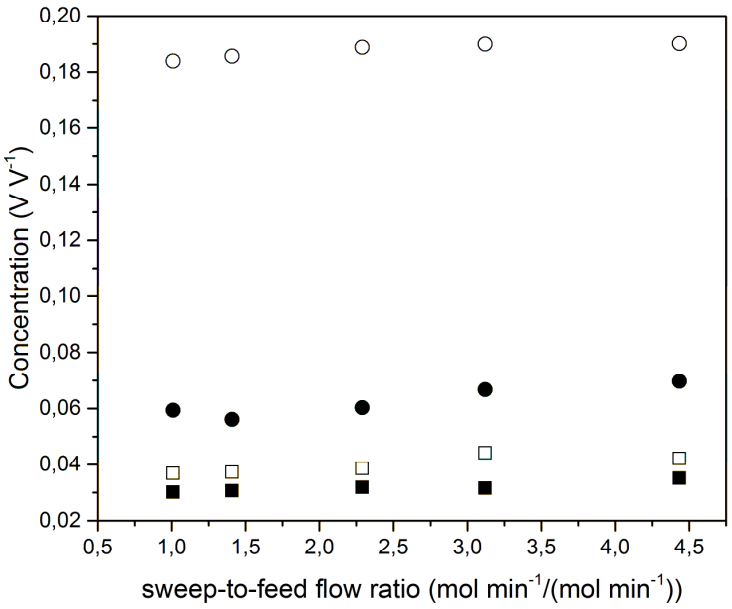

Fig. 13. O_2 concentration in permeate (○) and retentate (●). H_2O concentration in permeate (□) and retentate (■).(Temperature = 30-40°C, Feed pressure = 1.02 bar, Sweep/feed ratio = 1-3, flowrate of feed = 11.2 kg/h, using air as sweep gas)

The results in Fig. 13 show that all concentrations were only slightly affected by the increase of sweep-to-feed flow ratio. The increase of permeate O_2 and permeate H_2O could be explained by considering the corresponding permeate CO_2 decrease at the same sweep-to-feed flow ratios. Besides, the O_2 driving force (O_2 differential partial pressure) in the transport across the hollow fibres should support the O_2 movement from the shell to the lumen side of the module. The greater sweep flow rate decreased the time of O_2 and membrane contact. On the other hand, this could be compared to a reverse-sweep-to-feed ratio decrease for the O_2 that has a driving force to cross the membrane from the sweep to the feed side. The

decrease of this reverse ratio leads to a negative effect on the component transport. Water vapour and nitrogen displayed negligible movement as a consequence of their small driving force.

4. Conclusions

Through permeation tests it was possible to evaluate the gas separation performance of a bench-scale PDMS membrane module for the separation of CO_2/N_2 binary model mixtures. Measurements at different pressures, different feeding concentrations (5. 10, 15 and 20% CO_2) and with nitrogen as sweep gas revealed an average carbon dioxide permeability of 2943 ± 4.1%$_{RSD}$ Barrer. The bench-scale membrane module showed high potential to separate the binary mixture. The permeability was slightly affected by feed pressures ranging from 1 to 2.4 bar. Furthermore, the separation selectivity for a CO_2/N_2 mixture of 10%/90% (by volume) reached a maximum of 10.55 at 1.8 bar. Using information from the bench-scale experiments, a pilot-scale PDMS membrane module was investigated for the first time. A real flue gas was treated at 1 bar and 40°C, using air as sweep gas and varying sweep-to-feed flow ratio from 1 to 4.43. The concentration measurements and the CO_2 recovery showed that movement of other components across the membrane needed to be carefully considered. In real systems, oxygen from the air used as sweep gas, and water vapour from the combustion, in particular, would affect the CO_2 separation. Therefore, further investigations are needed on the influence of O_2 and H_2O on the separation. At the same time, experiments using the CO_2-enriched incoming combustion air need to be carried out in order to address the experimental study of the S-EGR system, and the impact that the transfer of oxygen leaving the sweep gas stream would have on the burner performance.

References

[1] Intergovernmental Panel on Climate Change, T.F. Stocker, D. Qin, G.-K. Plattner, M.M.B. Tignor, S.K. Allen, et al., Climate Change 2013 - The Physical Science Basis, 2013. doi:10.1038/446727a.

[2] E.S.R.L. US Department of Commerce, NOAA, ESRL Global Monitoring Division - Global Greenhouse Gas Reference Network, (n.d.).

[3] IPCC, 2005: IPCC Special Report on Carbon Dioxide Capture and Storage. Metz, B., O. Davidson, H. C. de Coninck, M. Loos, and L. A. Meyer (eds.). Cambridge University Press, Cambridge, United Kingdom and New York, NY, USA, 442 pp

[4] F. Kern, J. Gaede, J. Meadowcroft, J. Watson, The political economy of carbon capture and storage: An analysis of two demonstration projects, Technological Forecasting and Social Change. 102 (2016) 250–260. doi:10.1016/j.techfore.2015.09.010.

[5] P. Fennel, B. Anthony, Calcium and Chemical Looping Technology for Power Generation and Carbon Dioxide (CO_2) Capture, Woodhead Publishing Series in Energy, 2015. doi:10.1016/B978-0-85709-243-4.00013-6.

[6] R. Stanger, T. Wall, R. Spörl, M. Paneru, S. Grathwohl, M. Weidmann, et al., Oxyfuel combustion for CO_2 capture in power plants, International Journal of Greenhouse Gas Control. 40 (2015) 55–125. doi:10.1016/j.ijggc.2015.06.010.

[7] G. Scheffknecht, L. Al-Makhadmeh, U. Schnell, J. Maier, Oxy-fuel coal combustion—A review of the current state-of-the-art, International Journal of Greenhouse Gas Control. 5 (2011) S16–S35. doi:10.1016/j.ijggc.2011.05.020.

[8] R. Pardemann, B. Meyer, R. Pardemann, B. Meyer, Pre-Combustion Carbon Capture, in: Handbook of Clean Energy Systems, John Wiley & Sons, Ltd, Chichester, UK, 2015: pp. 1–28. doi:10.1002/9781118991978.hces061.

[9] A. Padurean, C.-C. Cormos, P.-S. Agachi, Pre-combustion carbon dioxide capture by gas–liquid absorption for Integrated Gasification Combined Cycle power plants, International Journal of Greenhouse Gas Control. 7 (2012) 1–11. doi:10.1016/j.ijggc.2011.12.007.

[10] K.E. Zanganeh, A. Shafeen, A novel process integration, optimization and design approach for large-scale implementation of oxy-fired coal power plants with CO_2 capture, International Journal of Greenhouse Gas Control. 1 (2007) 47–54. doi:10.1016/S1750-5836(07)00035-7.

[11] X. Fan, X. Fan, Post-Combustion Carbon Capture, in: Handbook of Clean Energy Systems, John Wiley & Sons, Ltd, Chichester, UK, 2015: pp. 1–30. doi:10.1002/9781118991978.hces024.

[12] T.C. Merkel, H. Lin, X. Wei, R. Baker, Power plant post-combustion carbon dioxide capture: An opportunity for membranes, Journal of Membrane Science. 359 (2010) 126–139. doi:10.1016/j.memsci.2009.10.041.

[13] R. Steeneveldt, B. Berger, T.A. Torp, CO_2 Capture and Storage: Closing the Knowing–Doing Gap, Chemical Engineering Research and Design. 84 (2006) 739–763. doi:10.1205/cherd05049.

[14] C.-H. Yu, C.-H. Huang, C.-S. Tan, A Review of CO_2 Capture by Absorption and Adsorption, Aerosol and Air Quality Research. 12 (2012) 745–769. doi:10.4209/aaqr.2012.05.0132.

[15] S. Choi, J.H. Drese, C.W. Jones, Adsorbent Materials for Carbon Dioxide Capture from Large Anthropogenic Point Sources, ChemSusChem. 2 (2009) 796–854. doi:10.1002/cssc.200900036.

[16] R. Ben-Mansour, M.A. Habib, O.E. Bamidele, M. Basha, N.A.A. Qasem, A. Peedikakkal, et al., Carbon capture by physical adsorption: Materials, experimental investigations and numerical modeling and simulations – A review, Applied Energy. 161 (2016) 225–255. doi:10.1016/j.apenergy.2015.10.011.

[17] D. Aaron, C. Tsouris, Separation of CO_2 from Flue Gas: A Review, http://dx.doi.org/10.1081/SS-200042244. (2011).

[18] E. Favre, Membrane processes and postcombustion carbon dioxide capture: Challenges and prospects, Chemical Engineering Journal. 171 (2011) 782–793. doi:10.1016/j.cej.2011.01.010.

[19] M. Mitrović, A. Malone, Carbon capture and storage (CCS) demonstration projects in Canada, Energy Procedia. 4 (2011) 5685–5691. doi:10.1016/j.egypro.2011.02.562.

[20] D. Best, B. Beck, Status of CCS development in China, Energy Procedia. 4 (2011) 6141–6147. doi:10.1016/j.egypro.2011.02.622.

[21] P.G. Cifre, K. Brechtel, S. Hoch, H. García, N. Asprion, H. Hasse, et al., Integration of a chemical process model in a power plant modelling tool for the simulation of an amine based CO_2 scrubber, Fuel. 88 (2009) 2481–2488. doi:10.1016/j.fuel.2009.01.031.

[22] S. Linnenberg, U. Liebenthal, J. Oexmann, A. Kather, Derivation of power loss factors to evaluate the impact of postcombustion CO_2 capture processes on steam power plant performance, Energy Procedia. 4 (2011) 1385–1394. doi:10.1016/j.egypro.2011.02.003.

[23] M. Mofarahi, Y. Khojasteh, H. Khaledi, A. Farahnak, Design of CO_2 absorption plant for recovery of CO_2 from flue gases of gas turbine, Energy. 33 (2008) 1311–1319. doi:10.1016/j.energy.2008.02.013.

[24] J. Franz, S. Schiebahn, L. Zhao, E. Riensche, V. Scherer, D. Stolten, Investigating the influence of sweep gas on CO_2/N_2 membranes for post-combustion capture, International Journal of Greenhouse Gas Control. 13 (2013) 180–190. doi:10.1016/j.ijggc.2012.12.008.

[25] M. Mulder, Basic Principles of Membrane Technology, Springer Netherlands, Dordrecht, 1996. doi:10.1007/978-94-009-1766-8.

[26] K.L. Wang, S.H. McCray, D.D. Newbold, E.L. Cussler, Hollow fiber air drying, Journal of Membrane Science. 72 (1992) 231–244. doi:http://dx.doi.org/10.1016/0376-7388(92)85051-J.

[27] Y. Zhang, J. Sunarso, S. Liu, R. Wang, Current status and development of membranes for CO_2/CH_4 separation: A review, International Journal of Greenhouse Gas Control. 12 (2013) 84–107. doi:10.1016/j.ijggc.2012.10.009.

[28] R.W. Baker, K. Lokhandwala, R.W. Baker, K. Lokhandwala, Natural Gas Processing with Membranes : An Overview Natural Gas Processing with Membranes : An Overview, 47 (2008) 2109–2121. doi:10.1021/ie071083w.

[29] R.A. Simonet, Methane recovery from landfill gas in order to produce natural gas by means of membranes, Desalination. 53 (1985) 289–295. doi:10.1016/0011-9164(85)85068-2.

[30] M.T. Ho, G.W. Allinson, D.E. Wiley, Reducing the Cost of CO_2 Capture from Flue Gases Using Membrane Technology, Industrial & Engineering Chemistry Research. 47 (2008) 1562–1568. doi:10.1021/ie070541y.

[31] R.W. Baker, J.G. Wijmans, T.C. Merkel, H. Lin, R. Daniels, and S. Thompson, "Gas Separation Processes Using Membranes with Permeate Sweep to Remove CO_2 from Combustion Gases," US Patent Number 7,964,020 B2 (June 21, 2011)

[32] P. Bernardo, E. Drioli, G. Golemme, Membrane Gas Separation: A Review/State of the Art, Industrial & Engineering Chemistry Research. 48 (2009) 4638–4663. doi:10.1021/ie8019032.

[33] C. Charmette, J. Sanchez, P. Gramain, A. Rudatsikira, Gas transport properties of poly(ethylene oxide-co-epichlorohydrin) membranes, Journal of Membrane Science. 230 (2004) 161–169. doi:10.1016/j.memsci.2003.10.043.

[34] T. Nakagawa, T. Nishimura, A. Higuchi, Morphology and gas permeability in copolyimides containing polydimethylsiloxane block, Journal of Membrane Science. 206 (2002) 149–163. doi:10.1016/S0376-7388(01)00775-X.

[35] P. Tremblay, M.M. Savard, J. Vermette, R. Paquin, Gas permeability, diffusivity and solubility of nitrogen, helium, methane, carbon dioxide and formaldehyde in dense polymeric membranes using a new on-line permeation apparatus, Journal of Membrane Science. 282 (2006) 245–256. doi:10.1016/j.memsci.2006.05.030.

[36] X. Feng, J. Ivory, Development of hollow fiber membrane systems for nitrogen generation from combustion exhaust gas, Journal of Membrane Science. 176 (2000) 197–207. doi:10.1016/S0376-7388(00)00445-2.

[37] A. Lindbråthen, M.-B. Hägg, CO_2 Capture from Natural Gas Fired Power Plants by Using Membrane Technology, Industrial & Engineering Chemistry Research. 44 (2005) 7668–7675. doi:10.1021/ie050174v.

[38] R. Bounaceur, N. Lape, D. Roizard, C. Vallieres, E. Favre, Membrane processes for post-combustion carbon dioxide capture: A parametric study, Energy. 31 (2006) 2220–2234. doi:10.1016/j.energy.2005.10.038.

[39] T.C. Merkel, X. Wei, Z. He, L.S. White, J.G. Wijmans, R.W. Baker, Selective exhaust gas recycle with membranes for CO_2 capture from natural gas combined cycle power plants, Industrial and Engineering Chemistry Research. 52 (2013) 1150–1159. doi:10.1021/ie302110z.

[40] H. Zhai, E.S. Rubin, Techno-economic assessment of polymer membrane systems for postcombustion carbon capture at coal-fired power plants, Environmental Science and Technology. 47 (2013) 3006–3014. doi:10.1021/es3050604.

[41] M. Ajhar, S. Bannwarth, K.-H. Stollenwerk, G. Spalding, S. Yüce, M. Wessling, et al., Siloxane removal using silicone–rubber membranes, Separation and Purification Technology. 89 (2012) 234–244. doi:10.1016/j.seppur.2012.01.003.

[42] P. Jha, L.W. Mason, J. Douglas Way, Characterization of silicone rubber membrane materials at low temperature and low pressure conditions, Journal of Membrane Science. 272 (2006) 125–136. doi:10.1016/j.memsci.2005.07.039.

[43] T.. Merkel, R.. Gupta, B.. Turk, B.. Freeman, Mixed-gas permeation of syngas components in poly(dimethylsiloxane) and poly(1-trimethylsilyl-1-propyne) at elevated temperatures, Journal of Membrane Science. 191 (2001) 85–94. doi:10.1016/S0376-7388(01)00452-5.

[44] C.K. Yeom, S.H. Lee, J.M. Lee, Study of transport of pure and mixed CO_2/N_2 gases through polymeric membranes, Journal of Applied Polymer Science. 78 (2000) 179–189. doi:10.1002/1097-4628(20001003)78:1<179::AID-APP220>3.0.CO;2-Z.

[45] M.K. Barillas, R.M. Enick, M. O'Brien, R. Perry, D.R. Luebke, B.D. Morreale, The CO_2 permeability and mixed gas CO_2/H_2 selectivity of membranes composed of CO_2-philic polymers, Journal of Membrane Science. 372 (2011) 29–39. doi:10.1016/j.memsci.2011.01.028.

[46] C.A. Scholes, S.E. Kentish, G.W. Stevens, Carbon Dioxide Separation through Polymeric Membrane Systems for Flue Gas Applications, Recent Patents on Chemical Engineering. 1 (2008) 52–66. doi:10.2174/2211334710801010052.

[47] J.E. Ramírez-Morales, E. Tapia-Venegas, N. Nemestóthy, P. Bakonyi, K. Bélafi-Bakó, G. Ruiz-Filippi, 2013, 'Evaluation of two gas membrane modules for fermentative hydrogen separation' International Journal of Hydrogen Energy, vol 38, no. 32, pp. 14042-14052. DOI: 10.1016/j.ijhydene.2013.08.092.

[48] M. Sadrzadeh, M. Amirilargani, K. Shahidi, T. Mohammadi, Gas permeation through a synthesized composite PDMS/PES membrane, Journal of Membrane Science. 342 (2009) 236–250. doi:10.1016/j.memsci.2009.06.047.

[49] S. Alexander Stern, Polymers for gas separations: the next decade, Journal of Membrane Science. 94 (1994) 1–65. doi:10.1016/0376-7388(94)00141-3.

[50] T.C. Merkel, V.I. Bondar, K. Nagai, B.D. Freeman, I. Pinnau, Gas sorption, diffusion, and permeation in poly(dimethylsiloxane), Journal of Polymer Science Part B: Polymer Physics. 38 (2000) 415–434. doi:10.1002/(SICI)1099-0488(20000201)38:3<415::AID-POLB8>3.0.CO;2-Z.

[51] R.C. Reid, J.M. Prausnitz, B.E. Poling, The Properties of Gases and Liquids, McGraw-Hill, New York, 1987, (n.d.).

[52] A. Brunetti, E. Drioli, Y.M. Lee, G. Barbieri, Engineering evaluation of CO_2 separation by membrane gas separation systems, Journal of Membrane Science. 454 (2014) 305–315.